IBRO Neuroscience Reports 21 (2026) 955–962

Contents lists available at ScienceDirect

IBRO Neuroscience Reports

journal homepage: www.sciencedirect.com/journal/IBRO-Neuroscience-Reports

Blood-brain barrier junctional proteins as potential biomarkers of cerebral ischaemia and reperfusion injury

Meaad Almusined [a], Pragati Kakkar [a], Nadira Y. Yuldasheva [a], Hema Viswambharan [a], Tarun Kakkar [b], Sikha Saha [a,*]

[a] Leeds Institute of Cardiovascular and Metabolic Medicine, Faculty of Medicine & Health, University of Leeds, Leeds, LS2 9JT, United Kingdom
[b] School of Chemical and Process Engineering, University of Leeds, Leeds, LS2 9JT, United Kingdom

ARTICLE INFO

Keywords:
Blood-brain barrier
Brain ischaemia
Stroke
Biomarker
Tight junction protein

ABSTRACT

Background: Cerebral ischaemia/reperfusion (CI/R) damage involves obstructing the blood supply to the brain, followed by restoring cerebral circulation through thrombolytic treatment. The blood-brain barrier (BBB) is a specialised structure separating the brain from peripheral blood circulation and plays an important role in brain function. However, little is known about CI/R-induced BBB damage and changes in circulatory biomarkers.
Methods and results: This novel study aims to examine the changes in BBB tight-junctional (TJ) proteins (Zonula occludens-1, Occludin and Claudin-5) in the hippocampus of the brain and determine the levels of these proteins in a mouse model of CI/R induced by bilateral common carotid occlusion. Expressions of BBB TJ proteins in the hippocampus were examined by immunohistochemistry and Western blotting. The levels of these proteins in blood serum were measured by Enzyme-Linked Immunosorbent Assay.
Conclusion: The results showed a significant decrease in BBB TJ proteins in the hippocampus, with increased levels of these proteins in blood serum in ischaemic mice as compared to sham-operated mice suggesting that these proteins can be used as potential biomarkers for the diagnosis of CI/R injury.

1. Introduction

Cerebral ischaemia/reperfusion (CI/R) injury due to blockage of brain artery, followed by thrombolytic treatment by tissue plasminogen activator (tPA) or mechanical thrombectomy to restore blood flow in the brain, is characterised by a series of pathological events, including the blood-brain barrier (BBB) damage. Ischaemic patients with bilateral common carotid artery occlusion (BCCAO) have particularly poor prognosis as a result of a high subsequent ischaemic prevalence rate (66% in bilateral internal carotid artery occlusion and 71% in bilateral common carotid artery occlusion) (Lai et al., 2005). Following cerebral ischaemia, the BBB is damaged, releasing degraded proteins into the blood circulation. The BBB is formed by brain microvascular endothelial cells interconnected by tight junctions (TJs), which selectively exclude most blood-borne substances from entering the brain. Endothelial cells, in conjunction with their neighbouring cells, such as pericytes and astrocytes, are critical for maintaining the normal physiology and function of the BBB. BBB plays an important role in maintaining the microenvironment for normal brain function and signalling (Liebner et al., 2018). Several studies have found that following CI/R the BBB is rapidly broken down, leading to increased BBB permeability (Lo et al., 2003). BBB leakage may also indicate massive dysfunction of microvessels, which could lead to poor outcomes after CI/R (Jiang et al., 2018).

In the endothelial cells, the zonula occludens (ZO) belong to the large family of membrane-associated guanylate kinase (MAGUK)-like proteins and the actin cytoskeleton is involved in the regulation of the integrity of cytoplasmic TJs. ZO-1 is a well-known TJ protein, and its damage reflects the severity of the pathological change of the BBB (Jiao et al., 2015). Occludin, a member of the TJ proteins, is also a key structural component of the BBB that has become an important focus of research in BBB damage (Liu et al., 2012; Yuan et al., 2020). Liu et al. (2012) have

Abbreviations: BBB, blood-brain barrier; BCCAO, bilateral common carotid artery occlusion; CA1, 2, 3, cornu ammonis 1,2,3; CI/R, cerebral ischaemia and reperfusion; CNS, central nervous system; GFAP, glial fibrillary acidic protein; MAGUK, membrane-associated guanylate kinase; MCAO, middle cerebral artery occlusion; NeuN, neuronal-specific nuclear protein; PB, phosphate buffer; TJ, tight junction; WB, western blotting; ZO-1, zonula occludens-1.

* Correspondence to: Discovery and Translational Science Department, Leeds Institute of Cardiovascular and Metabolic Medicine, Faculty of Medicine & Health, University of Leeds, Leeds LS2 9JT, United Kingdom.
E-mail address: s.saha@leeds.ac.uk (S. Saha).

https://doi.org/10.1016/j.ibneur.2026.09.021
Received 8 July 2026; Accepted 30 September 2026
Available online 2 October 2026
2667-2421/© 2026 Published by Elsevier Inc. on behalf of International Brain Research Organization. This is an open access article under the CC BY-NC-ND license (http://creativecommons.org/licenses/by-nc-nd/4.0/).

observed a rapid loss of Occludin in the ischaemic cerebral microvessels in a rat ischaemic stroke model (Liu et al., 2012). Occludin degradation has been observed in both human and animal studies with cerebral ischaemia leading to BBB breakdown (Yuan et al., 2020). Claudin-5 is the most dominant isoform of the Claudin family that decreases paracellular small molecule diffusion (Lv et al., 2018; Haseloff et al., 2015). However, several studies have shown that claudin-5 concentration remained unchanged following the middle cerebral artery occlusion in rats (Pan et al., 2017; Shi et al., 2017).

During the reperfusion phase of CI/R injury, reactive hyperaemia and loss of cerebral autoregulation lead to the acute opening of BBB TJs (Sandoval and Witt, 2008).

Different biomarker panels have been investigated in determining molecular characteristics of human CI/R with variable results. However, a deeper investigation of CI/R-induced BBB damage is required for better diagnosis, prognosis, and early treatment of CI/R injury.

Earlier studies, including our group, have shown that transient BCCAO followed by reperfusion in mice produces consistent and reproducible brain injury in the hippocampus and neurological dysfunction (Jiao et al., 2015; Khan et al., 2018; Yuan et al., 2019). The present study aims to examine the changes in BBB TJ proteins in the hippocampus and determine the levels of these circulating biomarkers following CI/R injury in this optimised mouse BCCAO model.

2. Materials and methods

2.1. A murine model for cerebral ischaemia and reperfusion

All mouse procedures were approved by the University of Leeds project licence, according to the ARRIVE guidelines as specified in the U.K. Animals (Scientific Procedures) Act, 1986 and the European Communities Council Directive of 24 November 1986 (86/609/EEC).

All experiments were performed on 10–12-week-old (25–30 g) male C57Bl/6 J mice (n = 54) Harlan-Olac, Bicester, UK), according to the ARRIVE guidelines, as specified in the U.K. Animals (Scientific Procedures) Act, 1986 and European Communities Council Directive of 24 November 1986 (86/609/EEC).

The animals were housed under a 12 h/12 h light/dark cycle and were provided with pellet food and water *ad libitum* to provide post-ischaemic support in mice (Lourbopoulos et al., 2017; Kestner et al., 2020). CI/R in mice (n = 28) was induced by transient BCCAO, according to our previously published method (Khan et al., 2018). We induced a 15-minute BCCAO, followed by 5 days of reperfusion. This procedure leads to consistent cellular damage in the brains of ischaemic mice. Sham-operated mice (n = 26) underwent the same procedure, except that the carotid arteries were not occluded.

Neurological assessment was performed in BCCAO and sham-operated mice by neurological deficit signs, as published previously (Khan et al., 2018) i.e., 0, no observable deficit; 1, drowsiness and circling; 2, torsion of the neck and disappearance of the righting reflex; 3, seizure; 4, no spontaneous movement or coma. Two animals were excluded from our analysis due to incomplete occlusion.

2.2. Tissue processing for immunohistochemistry

Following 5 days of survival time, BCCAO and sham-operated mice were perfused transcardially with 4% paraformaldehyde in 0.1 M phosphate buffer (PB, pH 7.4). Brains were post-fixed in PB overnight and stored in 0.1 M phosphate buffer saline (PBS) at 4°C. Brain sections (20 μm) were cut using a cryostat (Leica, Bensheim, Germany) and processed for immunohistochemistry.

2.3. Primary antibody specificity

The specificities of antibodies were determined previously by the suppliers. In particular, an antibody against NeuN (Abcam, code number ab104224) was prepared by immunising mice with N N-terminal peptide 1B7. Antibody against glial fibrillary acidic protein (GFAP; Invitrogen, code number 131–17719) was prepared by immunising mice with 131–17719. An antibody against Occludin (Life Technologies, code number OC-3F10) was prepared by immunising mice with C C-terminal peptide OC-3F10. An antibody against ZO-1(Invitrogen, code number 40–2200) was prepared by immunising the rabbit with a synthetic peptide found in the ZO-1 protein's middle region. Antibody against Claudin-5 (Invitrogen, code number 34–1600) was prepared by immunising rabbits with synthetic peptides from the Claudin-5C-terminus.

2.4. Immunohistochemistry

The brain sections were placed in wells and treated with Liberate L.A.B. Solution (antigen retrieval solution, Polysciences Inc.) for 10 min to remove excessive fixative and minimise protein cross-linking. Sections were then washed with PBS containing 0.01% Triton-X100 (PBS-T) for 5 min, followed by incubation in 10% horse or donkey serum (Sigma-Aldrich, Poole, Dorset, UK) diluted in PBS-T at room temperature on a shaker (Bio Dancer, New Brunswick Scientific, Edison N.J USA) for 30 min with gentle agitation to block any non-specific binding and decrease background staining. Following that, sections were transferred to the appropriate primary antibodies. The primary antibodies used were NeuN (Abcam-ab104224), GFAP (Invitrogen-A21282), Occludin (Life Technologies-331511), Claudin-5 (Invitrogen-34–1600), ZO-1 (Invitrogen-40–2200), CD31 (Abcam-ab28364), and CD31 (Invitrogen-14–0311–82). Sections were incubated overnight with antibodies diluted in PBS-T and 10% horse serum at 40°C. The dilutions of these antibodies used were 1:4000 (NeuN), 1:1000 (GFAP), 1:50 (Occludin), 1:500 (Claudin-5), and 1:100 (ZO-1). Sections were washed three times for 5 min each on a shaker table with gentle agitation. Sections were then transferred to appropriate (rabbit or mouse) secondary antibodies conjugated with Cy3 (red fluorescence) (Jackson Immunosearch Laboratories-115–167–003) or Alexa488 (green fluorescence) (Jackson Immunoresearch Laboratories-115–545–003) (diluted 1:1000 in PBS-T with 10% horse serum), covered with foil and incubated at room temperature on the shaker table for 4 h. Finally, sections were washed three times each for 5 min, mounted on slides and cover-slipped using Vectashield mounting medium with or without DAPI (Vector Laboratories Inc., Burlingame, CA 94010).

The analysis of brain sections was carried out using Zeiss Axioskop 2 or AxioImager Z1 fluorescence microscopes. Multiple digital images were taken with the imaging system (Acquis (Axioskop 2) or an Axiovision (AxioImager Z1) for analysis.

2.5. Stereological method for quantification of immunolabelled profiles

Fifteen minutes of BCCAO followed by 5 days of reperfusion produces consistent and reproducible neuronal death and astrocyte activation in this region (Khan et al., 2018). The number of NeuN immunoreactive neuronal cells, GFAP immunoreactive glial cells and processes per unit volume of tissue in the hippocampus was estimated using a three-dimensional counting method, based on our previously published method (Khan et al., 2018).

2.6. Immunoblotting

Western blotting analysis was carried out in the hippocampal regions of the forebrain. In brief, the mice were sacrificed by decapitation under anaesthesia. Brains were removed and snap-frozen on dry ice. The hippocampal tissue samples (25–35 milligrams) from both sides of the brain were collected at the forebrain level corresponding to bregma −0.22 to −2.06 mm (Paxinos GFranklin, 2001) with a 1 mm corer under a 5x dissecting microscope, according to a previously published method (Khan et al., 2018; Ketheeswaranathan et al., 2011). The hippocampal tissues were homogenised using a Blunt 20-gauge blunt needle and

Table 1
Detection range, sensitivity and specificity for mouse ELISA kits used.

ELISA kit name and catalogue number	Detection range	Sensitivity	Specificity
Mouse GFAP ELISA Kit (Fine test, EM0335)	15.625 −1000 pg/ml	< 9.375 pg/ml	For quantitative detection of GFAP in serum, plasma, tissue homogenates and other biological fluids.
Mouse Occludin ELISA Kit (AVIVA Systems Biology, OKEH 07095),	0.156 – 10 ng/ml	< 0.078 ng/ml	Mouse Occludin UniProt ID: Q61146 GeneID: 18260 Target Alias: AI503564, Occludin, Ocl.
Mouse Claudin-5 ELISA kit (DL EVELOP, DL-CLDN5-Mu)	0.312–20 ng/ml	< 0.127 ng/ml	This assay has high sensitivity and excellent specificity for the detection of CLDN5.
Mouse TJP1 (Tight junction protien ZO-1) ELISA Kit (Elabscience, E-EL-M1161)	78.13–5000 pg/ml	46.88 pg/ml	This kit recognizes Mouse TJP1 in samples.

extracted using 300 microlitres of lysis buffer (ThermoFisher Scientific, 87787).

Harvested hippocampal tissues were homogenised and sonicated using the FB120 probe-sonicator from Fisher Scientific in an ice bath, twice at 5 s and centrifuged for 30 min at 13,000 rpm at 4°C, before estimating protein concentrations using the BCA assay (Pierce Protein Quantification Kit). Equal amounts of cytosolic protein were resolved on 12% SDS polyacrylamide gels (Invitrogen) and transferred to polyvinylidene difluoride membranes (Millipore) and incubated for 1 h in TBS-T (Tris-buffered saline and 0.1% Tween 20) containing 5% non-fat milk. Membranes were then immunoblotted and incubated overnight at 4°C with appropriate primary antibodies: GFAP, ZO-1, Occludin and Claudin-5 (diluted 1:1000) against beta-Actin (1:1000). Membranes were washed in TBS-T three times (15 min) on a shaker and incubated for 1 h at room temperature with corresponding HRP-conjugated anti-rabbit or anti-mouse antibodies (Santa Cruz Biotechnology; 1:1000). The membranes were washed in TBS-T once for 15 min and incubated in Anti-western-C marker (Streptactin) (BIO-RAD) diluted in TBS-T (1:25,000) for 10 min. The membranes were washed in TBS-T twice (15 min each). The membranes were developed with the Immobion Western HRP substrate luminol reagent with peroxide reagent (Millipore). The Syngene densitometry (Syngene Gel Documentation) system was used to quantify the immunoblots. Densitometric quantification analysis of blots was performed using GeneTools analysis software along with Excel software.

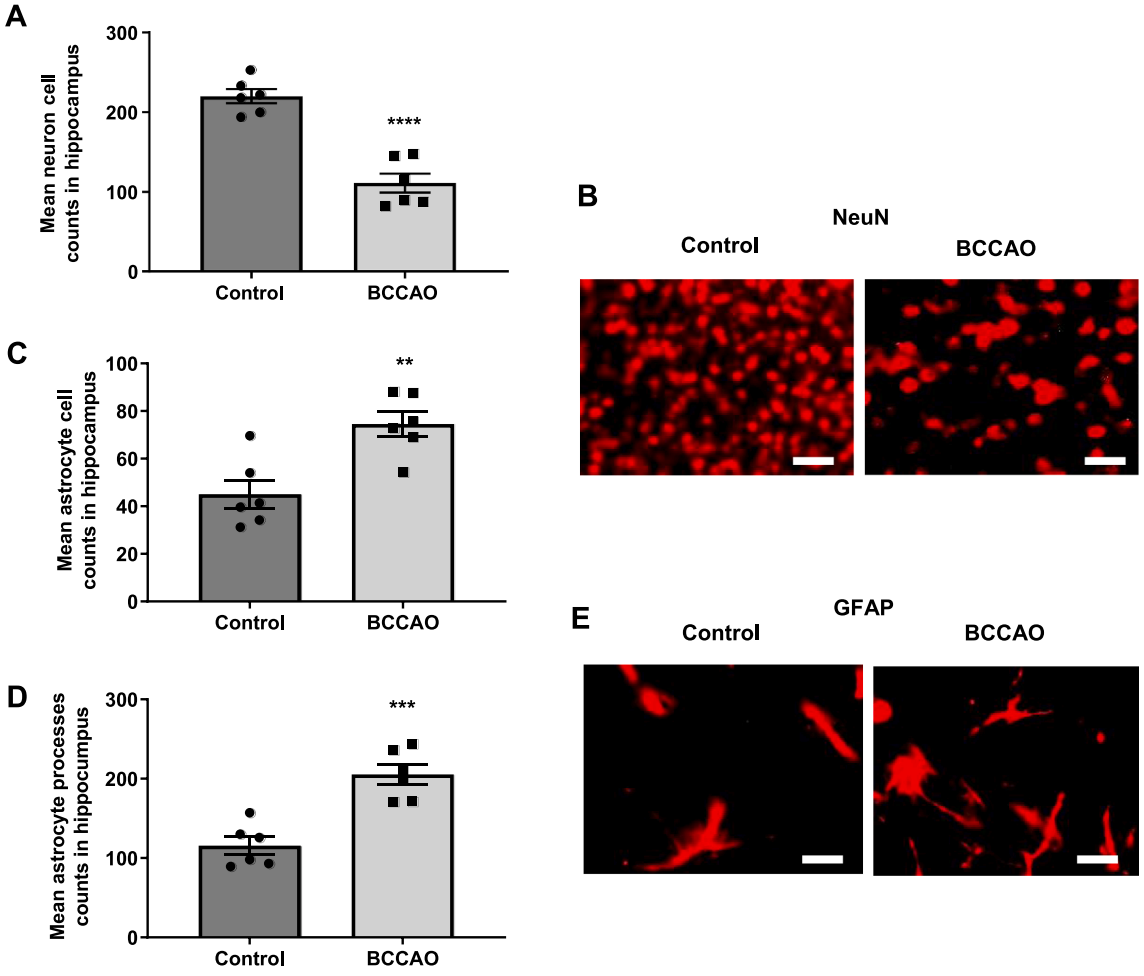


Fig. 1. Neuronal death and changes in astrocytes following BCCAO. Quantitative analysis shows significant differences in the number of (A) NeuN-positive cells and (C and D) GFAP labelled astrocyte cells and processes in the hippocampus of sham-operated and stroke mice (n = 6). **p < 0.01; ***p < 0.001, ****p < 0.0001 unpaired student *t*-test. Data are represented as mean ± SEM. Representative photomicrographs showing immunofluorescence staining of (B) NeuN-labelled cells and (E) GFAP-labelled astrocytes in the hippocampus in control and stroke (n = 6). Scale bars: 20 μm and the images are taken at the level of Bregma −2.06 mm.

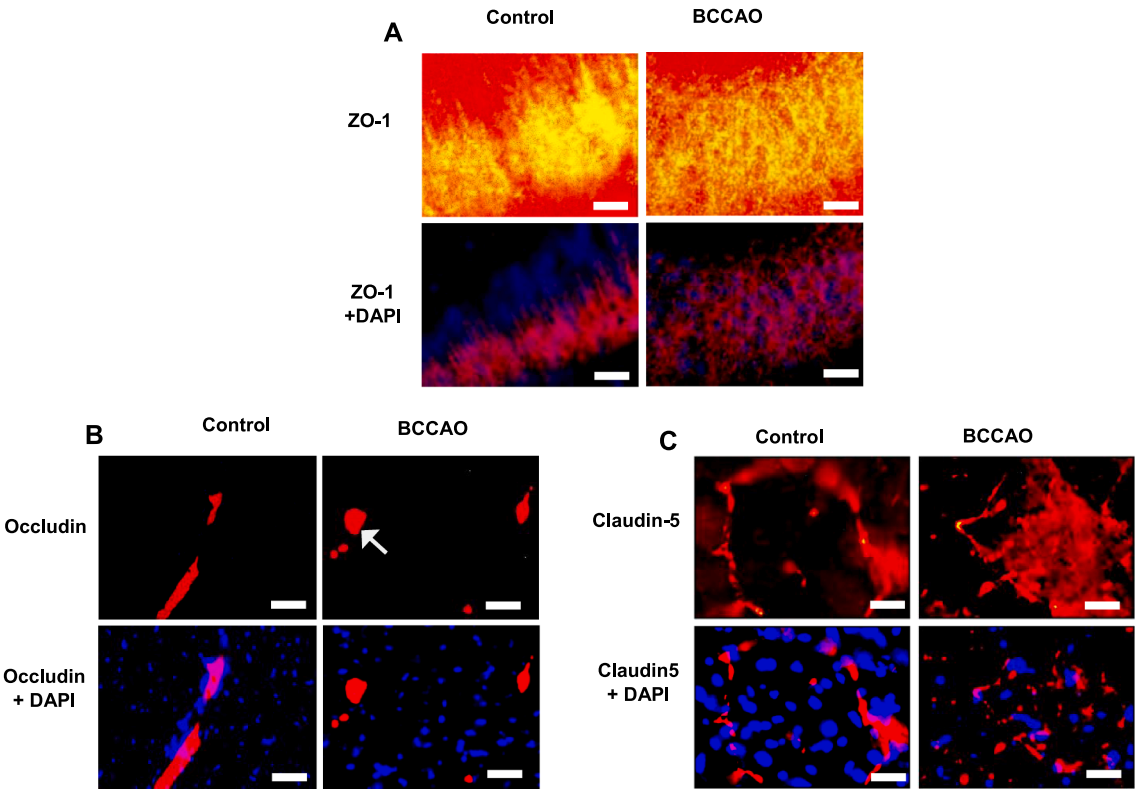


Fig. 2. Changes in TJ proteins following BCCAO. Representative photomicrographs showing immunofluorescence staining for (A) ZO-1 with anti-ZO-1, (B) Occludin with anti-Occludin, and (C) Claudin-5 with anti-Claudin-5, and DAPI-labelled nuclei in the hippocampus of control and BCCAO mice brains (n = 3). The labelled TJs are disrupted in the BCCAO brain (arrows) compared to the intact TJs in the control (arrows). Scale bar= 10 μm and the images are taken at the level of Bregma-2.06 mm.

2.7. Analysis and measurement of blood biomarkers using the ELISA method

Blood samples were collected in a gel clot active tube (Gold Hemogard closure) from the inferior vena cava from 8 BCCAO and 8 sham-operated mice (~1 ml blood from each mouse). Blood samples were collected after 5 days of BCCAO and the sham operation. The blood samples were centrifuged (Bifug Pico) at 1500 g for 10 mins within two hours of collection. Samples were then flash-frozen in liquid nitrogen and stored in a freezer at −80°C until analysis. For measurement of blood biomarkers, mouse GFAP ELISA Kit (Fine test, EM0335), mouse Occludin ELISA Kit (AVIVA Systems Biology, OKEH 07095), mouse Claudin-5 ELISA kit (DL EVELOP, DL-CLDN5-Mu) and mouse TJP1 (Tight junction protein ZO-1) ELISA Kit (Elabscience, E-EL-M1161) were used, and the protocols were followed according to manufacturers' guidance. Table 1 shows the detection range, sensitivity and specificity for each previously mentioned ELISA kit. In brief, 100 microlitres of the serially diluted standards and serum samples with control (zero) solutions were added to each well and incubated for 90 min in GFAP and ZO-1 assays and 2 h in Occludin and Claudin-5 assays at 37°C. Then, the liquid was removed, and 100 microlitres of Biotin-conjugated antibody was added to each well for 60 min at 37°C. Subsequently, the plate was washed three times, and 100 microlitres of HRP Conjugate (SABC) was added to each well and incubated for 30 min in GFAP, Occludin and ZO-1 assay and 1 h in Claudin-5 assay at 37°C. The plate was then washed five times, and 90 microlitres of TMB substrate was added to each well for 15 min at 37°C. Finally, 50 μL of Stop Solution was added, followed by optimal density determination, immediately at 450 nm with a plate reader.

2.8. Statistical analysis

Data were shown as mean ± SEM. Excel program and GraphPad Prism 9 software (GraphPad, San Diego, California) were used for statistical analysis and visualisation. Normality tests were carried out routinely. A value of $p < 0.05$ was considered statistically significant by the Mann-Whitney *U* test. Quantification of immunolabelled profile data was analysed using an unpaired *t*-test to determine statistical significance, and a multiple comparison test was used for post-hoc comparisons.

3. Results

3.1. Immunohistochemical analysis of immunoreactive cells and profiles

NeuN, a neuronal-specific nuclear protein that is commonly used as a marker of mature neurons (Gusel'Nikova and Korzhevskiy, 2015), was used to determine the extent of neuronal death in the hippocampus. Antibodies to GFAP, an intermediate filament protein that is predominantly expressed by astrocytes, were used to label changes in glial cells and processes following CI/R. The results showed that 15 min of ischaemia and 5 days of reperfusion induced considerable loss of NeuN-labelled neurones (Fig. 1 A, B) and increase in GFAP-positive glial cells and processes (Fig. 1 C, D, E) in the hippocampus, confirming our previous study, where detailed analyses were performed to assess neuronal death and changes in glial cells and processes in the hippocampal subfields CA1, CA2 and CA3 (Khan et al., 2018).

Qualitative immunohistochemical analysis showed ZO-1 (Fig. 2A), Occludin (Fig. 2B), and Claudin-5 (Fig. 2C) expressions were reduced in the hippocampus of the BCCAO mice compared to sham-operated mice.

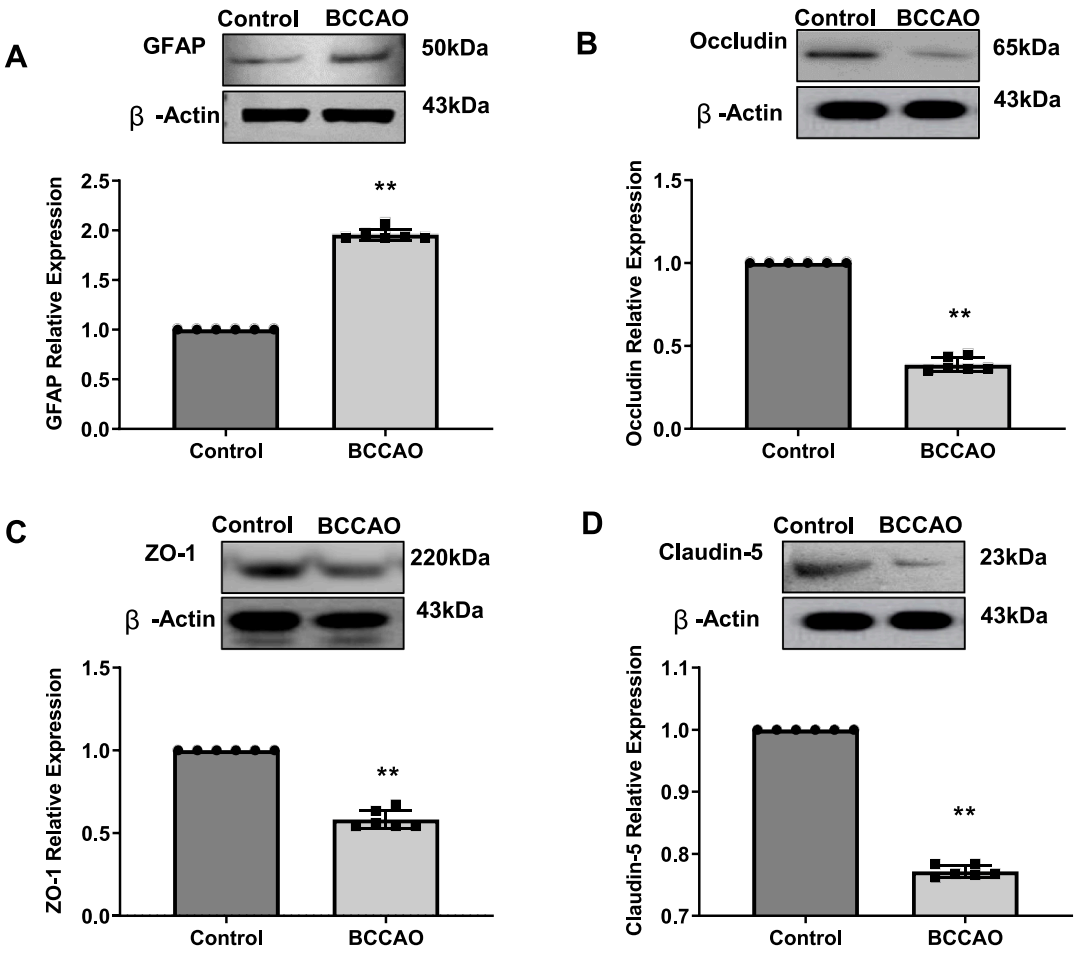


Fig. 3. WB analysis of protein expressions following BCCAO. Western blotting (WB) analysis of (A) GFAP, (B) Occludin, (C) ZO-1 and (D) Claudin-5 expressions in the hippocampus of sham-operated and BCCAO mice (n = 6). ß-actin was used as a loading control. **p < 0.01, Mann-Whitney *U* test and data presented as mean ± SD. The control group was set as 1 in comparison to the BCCAO group.

3.2. Immunoblotting analysis of protein expression after ischaemia/reperfusion

Quantitative Western Blotting (WB) analysis of GFAP expression in hippocampus tissues showed a significant increase in GFAP protein in the hippocampus of ischaemic mice compared to the control mice (Mann-Whitney *U* test, p = 0.0022, Fig. 3A), consistent with the observed immunostaining data. The expression levels of the BBB TJs proteins in the hippocampus of the BCCAO mice were significantly lower (Occludin, p = 0.0022, Fig. 3B; ZO-1, p = 0.0022, Fig. 3C; and Claudin-5, p = 0.0022, Fig. 3D) compared to the sham-operated mice, confirming our qualitative immunohistochemical results. The expression levels of all three TJ proteins were reduced significantly in the hippocampus following CI/R, confirming disruption of BBB integrity, as determined by immunohistochemistry.

3.3. Analysis of markers in blood serum

The serum levels of GFAP, ZO-1, Occludin, and Claudin-5 from BCCAO and sham-operated mice were quantified using Enzyme-Linked Immunosorbent Assay (ELISA). The quantitative statistical analysis showed a significant increase of 1.5-fold in GFAP level (Control vs BCCAO, 116.8 ± 13.8 vs 182.1 ± 34.6; p = 0.0002, Fig. 4A), a 1.34-fold increase in Occludin level (Control vs BCCAO, 181 ± 6.7 vs 243 ± 11.1; p < 0.0001, Fig. 4B), a 3-fold increase in the ZO-1 level (Control vs BCCAO, 527.9 ± 125.4 vs 1595 ± 337.4; p < 0.0001, Fig. 4C) and ~ 3.6-fold increase in the level of Claudin-5 (Control vs BCCAO, 278.3 ± 30.4 vs 1028 ± 96.5; p < 0.0001, Fig. 4D) in the ischaemic group of mice compared to the sham-operated mice.

4. Discussion

The present study is the first systematic study investigating detailed changes in BBB junctional proteins (ZO-1, Occludin, Claudin-5) in the hippocampus in the brain following CI/R induced by BCCAO and reperfusion in C57Bl/6 J mice. This novel study also quantifies these protein concentrations in the blood serum of ischaemic mice, suggesting that these proteins could be used as potential biomarkers of CI/R.

Our previous study (Khan et al., 2018) along with others (Murakami et al., 1998; Yang et al., 1997) showed that transient BCCAO in these mice developed consistent and selective neuronal death in the hippocampal subfields, CA1, CA2 and CA3 and motor, somatosensory and insular cortex, with a higher survival rate.

Quantitative immunohistochemical analysis showed a significant increase in GFAP-labelled astrocyte processes and cells following CI/R in the hippocampus, confirming our previous study (Khan et al., 2018). The results also confirmed studies that reported the altered morphology of astrocytes after cerebral ischaemia is related to the increased expression of GFAP (Lebkuechner et al., 2015; Sofroniew, 2009). GFAP up-regulation is one of the most important features of astrogliosis (an abnormal increase in the astrocyte number following CI/R) (Pekny et al., 1999). Astrocyte processes identified by GFAP immunostaining in the hippocampus of the BCCAO mice appeared to be rearranged and have become thicker, an indication of reactive gliosis (Burda and Sofroniew,

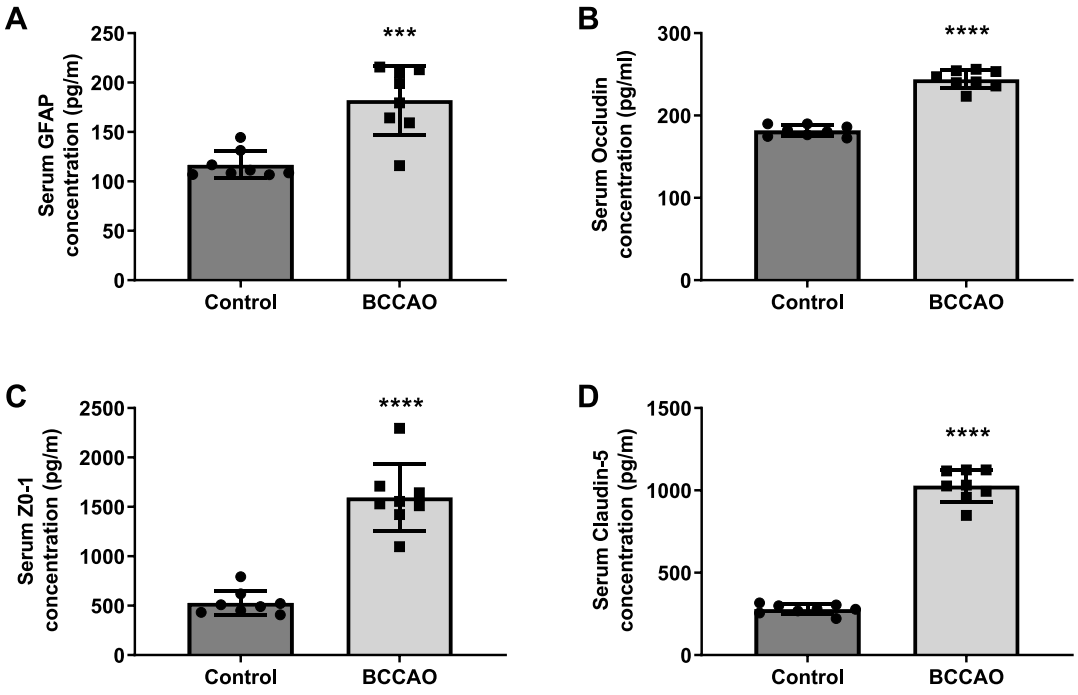


Fig. 4. Analysis of biomarkers in serum. Serum levels of (A) GFAP, (B) Occludin, (C) ZO-1, and (D) Claudin-5 in control and BCCAO stroke mice (n = 8). A significant difference in the serum levels of biomarkers in control and BCCAO mice (A: GFAP, $p = 0.0002$), (B: Occludin, $p < 0.0001$), (C: ZO-1, $p < 0.0001$) and (D: Claudin-5, $p < 0.0001$). ***$p < 0.001$, ****$p < 0.001$ unpaired student *t*-test.

2014; Pekny and Nilsson, 2005). This may contribute to central nervous system dysfunction, including maladaptive synaptic plasticity in the glial-neuronal network, leading to abnormal synaptic transmission (Papa et al., 2014). Increased level of GFAP in blood in mice following CI/R observed in the present study confirmed previous clinical studies that investigated the role of serum GFAP as a diagnostic tool by showing increased level of circulatory GFAP in ischaemic patients (Luger et al., 2017; Schiff et al., 2012).

The present study demonstrated disruption of BBB TJ proteins (ZO-1, Occludin and Claudin-5) in the CI/R brain compared to the sham brain. The significant reduction in TJ protein expressions in the hippocampus was reported previously in the rat brain following middle cerebral artery occlusion (MCAO) (Ren et al., 2015; Yang and Rosenberg, 2011). However, to our knowledge, it is the first study in the mouse BCCAO model. The present study, for the first time, reported significant increases in these three TJ proteins in the blood serum in CI/R mice compared to the control mice. The increased concentrations of these three TJ proteins in blood serum reflected the disarrangements and reductions of these proteins in the brain following CI/R.

ZO-1 is one of the main TJ proteins that reduce cerebral vessel permeability by restricting the free molecular exchange between blood and brain tissues (Itoh and Bissell, 2003). Previous studies using brain microvessel endothelial cells showed that dissociation of ZO-1 from the TJs complex has been linked to increased permeability of the BBB, suggesting that the ZO-1-transmembrane protein connection is crucial for the stability and function of the BBB (Mark and Davis, 2002; Fischer et al., 2002).

Increased serum level of Occludin after BCCAO-induced CI/R in mice observed in the present study also confirmed previous works in a rat model of MCAO and reperfusion (Pan et al., 2017; Liu et al., 2018). Occludin is also one of the main TJ proteins that is an integral part of the BBB structure (Hawkins and Davis, 2005). Changes in the Occludin expression in the brain are reported to be linked to the disruption in the regulatory mechanisms of the BBB (Sandoval and Witt, 2008). We observed disruption of Claudin-5 expression in the hippocampus and an increased level of Claudin-5 in the blood serum of ischaemic mice compared to the sham-operated mice. However, earlier studies in a rat model of MCAO reported that the blood level of Claudin-5 did not change considerably during the first 4.5 h (Liu et al., 2012). We used the mouse BCCAO model and did not determine the time course level of these proteins following CI/R, making it difficult to compare our results with earlier studies. Disruptions in Claudin-5 expression are linked to a large increase in paracellular solute permeability, as shown in a previous study in rats following MCAO (Liu et al., 2012). Claudin-5 has also been shown to be one of the integral components of the BBB TJs that control BBB permeability (Ohtsuki et al., 2007; Nitta et al., 2003).

Our data for the first time demonstrated reduction of specific BBB TJ proteins in the hippocampus together with increased circulatory levels of these proteins in a BCCAO model. However, the measurement of BBB permeability to assess functional changes in the BBB was beyond the scope of the study. The present study was also limited by the fact that the circulating BBB proteins were measured in a single model at a single time point, 5 days after reperfusion. Future studies on measurement of BBB permeability and assessment of BBB TJ proteins in different preclinical ischaemic models and human blood samples at different time points particularly in the acute phase of CI/R are important to understand the mechanisms of ischaemia-induced BBB damage and release of these proteins in circulation and their potential clinical diagnostic utility.

Nevertheless, this study provides valuable information on CI/R-induced changes in BBB proteins in the brain as well as in the circulation and represents an important step forward in investigating brain-derived proteins in blood serum following CI/R injury. However, more research is needed before implementing the BBB biomarker strategies in clinical CI/R scenarios.

5. Conclusion

Our novel data validate the occurrence of neuronal death and astrogliosis alongside disruptions in the BBB TJs in a murine model of

CI/R. The results suggest that the implementation of circulating BBB TJ markers alone or in combination with GFAP may be a promising approach for improving the precision of CI/R-induced BBB damage in patients' diagnosis. The results are also helpful for further understanding of the underlying mechanisms of CI/R and developing new diagnostic biomarker strategies and therapeutic approaches targeting the BBB. As discussed, these data, however, require validation in acute CI/R stage in other models, such as the mouse MCAO model and the efficiency of these biomarkers needs to be validated conclusively in clinical studies.

CRediT authorship contribution statement

Meaad Almusined: Writing – original draft, Formal analysis. **Pragati Kakkar:** Writing – review & editing. **Nadira Y. Yuldasheva:** Supervision. **Hema Viswambharan:** Supervision. **Tarun Kakkar:** Writing – review & editing. **Sikha Saha:** Writing – review & editing, Supervision, Methodology, Funding acquisition, Conceptualization.

Author contributions

MA conducted experimental work carried out data analysis and wrote the draft manuscript. PK helped with the immunohistochemical images, formatted the manuscript, and revised the references. NYY performed all surgical procedures. HV supervised the immunoblot experiments and data analysis. TK contributed to the immunohistochemical images. SS conceived and designed the study, supervised the experimental work, and proofread the manuscript with input from all authors.

Informed consent statement

Not applicable.

Ethics approval for experimental studies

The animal study protocol was approved by the Institutional Review Board (or Ethics Committee) of the U.K. Animals (Scientific Procedures) Act, 1986, and the European Communities Council Directive of 24 November 1986 (86/609/EEC). All experiments were performed on 10- to 12-week-old (25–30 g) male C57BL/6 J mice (Harlan-Olac, Bicester, UK) according to the ARRIVE guidelines. No human samples or subjects were used in this study.

Funding

This research is supported by a PhD scholarship from the "Research Center of the Female Scientific and Medical Colleges", Deanship of Scientific Research, King Saud University, Saudi Arabia.

This research is also supported by the Medical Research Council (MRC), UK (grant number MR/Y503460/1).

Declaration of Competing Interest

The authors declare that they have no known competing financial interests or personal relationships that could have appeared to influence the work reported in this paper.

Data availability

The datasets used and/or analysed during the current study are available from the corresponding author upon reasonable request.

References

Burda, J.E., Sofroniew, M.V., 2014. Reactive gliosis and the multicellular response to CNS damage and disease. Neuron 81, 229–248.
Fischer, S., Wobben, M., Marti, H., Renz, D., Schaper, W., 2002. Hypoxia-induced hyperpermeability in brain microvessel endothelial cells involves VEGF-mediated changes in the expression of zonula occludens-1. Microvasc. Res. 63, 70–80.
Gusel'Nikova, V., Korzhevskiy, D., 2015. NeuN as a neuronal nuclear antigen and neuron differentiation marker. Acta Nat. (англоязычная версия) 7, 42–47.
Haseloff, R.F., Dithmer, S., Winkler, L., Wolburg, H., Blasig, I.E., 2015. Transmembrane proteins of the tight junctions at the blood–brain barrier: structural and functional aspects. Proc. Semin. Cell Dev. Biol. 16–25.
Hawkins, B.T., Davis, T.P., 2005. The blood-brain barrier/neurovascular unit in health and disease. Pharmacol. Rev. 57, 173–185.
Itoh, M., Bissell, M.J., 2003. The organization of tight junctions in epithelia: implications for mammary gland biology and breast tumorigenesis. J. Mammary Gland. Biol. Neoplasia 8, 449–462.
Jiang, X., Andjelkovic, A.V., Zhu, L., Yang, T., Bennett, M.V., Chen, J., Keep, R.F., Shi, Y., 2018. Blood-brain barrier dysfunction and recovery after ischemic stroke. Progress. Neurobiol. 163, 144–171.
Jiao, X., He, P., Li, Y., Fan, Z., Si, M., Xie, Q., Chang, X., Huang, D., 2015. The role of circulating tight junction proteins in evaluating blood brain barrier disruption following intracranial hemorrhage. Dis. Markers 2015, 860120.
Kestner, R.-I., Mayser, F., Vutukuri, R., Hansen, L., Günther, S., Brunkhorst, R., Devraj, K., Pfeilschifter, W., 2020. Gene expression dynamics at the neurovascular unit during early regeneration after cerebral ischemia/reperfusion injury in mice. Front. Neurosci. 14, 280.
Ketheeswaranathan, P., Turner, N.A., Spary, E.J., Batten, T.F., McColl, B.W., Saha, S., 2011. Changes in glutamate transporter expression in mouse forebrain areas following focal ischemia. Brain Res. 1418, 93–103.
Khan, S., Yuldasheva, N.Y., Batten, T.F., Pickles, A.R., Kellett, K.A., Saha, S., 2018. Tau pathology and neurochemical changes associated with memory dysfunction in an optimised murine model of global cerebral ischaemia-A potential model for vascular dementia? Neurochem. Int. 118, 134–144.
Lai, S.-L., Chen, Y.-C., Weng, H.-H., Chen, S.-T., Hsu, S.-P., Lee, T.-H., 2005. Bilateral common carotid artery occlusion—a case report and literature review. J. Neurol. Sci. 238, 101–104.
Lebkuechner, I., Wilhelmsson, U., Möllerström, E., Pekna, M., Pekny, M., 2015. Heterogeneity of Notch signaling in astrocytes and the effects of GFAP and vimentin deficiency. J. Neurochem. 135, 234–248.
Liebner, S., Dijkhuizen, R.M., Reiss, Y., Plate, K.H., Agalliu, D., Constantin, G., 2018. Functional morphology of the blood–brain barrier in health and disease. Acta Neuropathol. 135, 311–336.
Liu, J., Jin, X., Liu, K.J., Liu, W., 2012. Matrix metalloproteinase-2-mediated occludin degradation and caveolin-1-mediated claudin-5 redistribution contribute to blood–brain barrier damage in early ischemic stroke stage. J. Neurosci. 32, 3044–3057.
Liu, P., Zhang, R., Liu, D., Wang, J., Yuan, C., Zhao, X., Li, Y., Ji, X., Chi, T., Zou, L., 2018. Time-course investigation of blood–brain barrier permeability and tight junction protein changes in a rat model of permanent focal ischemia. J. Physiol. Sci. 68, 121–127.
Lo, E.H., Dalkara, T., Moskowitz, M.A., 2003. Mechanisms, challenges and opportunities in stroke. Nat. Rev. Neurosci. 4, 399–414.
Lourbopoulos, A., Mamrak, U., Roth, S., Balbi, M., Shrouder, J., Liesz, A., Hellal, F., Plesnila, N., 2017. Inadequate food and water intake determine mortality following stroke in mice. J. Cereb. Blood Flow Metab. 37, 2084–2097.
Luger, S., Witsch, J., Dietz, A., Hamann, G.F., Minnerup, J., Schneider, H., Sitzer, M., Wartenberg, K.E., Niessner, M., Foerch, C., 2017. Glial fibrillary acidic protein serum levels distinguish between intracerebral hemorrhage and cerebral ischemia in the early phase of stroke. Clin. Chem. 63, 377–385.
Lv, J., Hu, W., Yang, Z., Li, T., Jiang, S., Ma, Z., Chen, F., Yang, Y., 2018. Focusing on claudin-5: a promising candidate in the regulation of BBB to treat ischemic stroke. Progress. Neurobiol. 161, 79–96.
Mark, K.S., Davis, T.P., 2002. Cerebral microvascular changes in permeability and tight junctions induced by hypoxia-reoxygenation. Am. J. Physiol. -Heart Circ. Physiol. 282, H1485–H1494.
Murakami, K., Kondo, T., Kawase, M., Chan, P.H., 1998. The development of a new mouse model of global ischemia: focus on the relationships between ischemia duration, anesthesia, cerebral vasculature, and neuronal injury following global ischemia in mice. Brain Res. 780, 304–310.
Nitta, T., Hata, M., Gotoh, S., Seo, Y., Sasaki, H., Hashimoto, N., Furuse, M., Tsukita, S., 2003. Size-selective loosening of the blood-brain barrier in claudin-5–deficient mice. J. Cell. Biol. 161, 653–660.
Ohtsuki, S., Sato, S., Yamaguchi, H., Kamoi, M., Asashima, T., Terasaki, T., 2007. Exogenous expression of claudin-5 induces barrier properties in cultured rat brain capillary endothelial cells. J. Cell. Physiol. 210, 81–86.
Pan, R., Yu, K., Weatherwax, T., Zheng, H., Liu, W., Liu, K.J., 2017. Blood occludin level as a potential biomarker for early blood brain barrier damage following ischemic stroke. Sci. Rep. 7, 40331.
Papa, M., De Luca, C., Petta, F., Alberghina, L., Cirillo, G., 2014. Astrocyte–neuron interplay in maladaptive plasticity. Neurosci. Biobehav. Rev. 42, 35–54.
Paxinos GFranklin, K., 2001. The mouse brain in stereotaxic coordinates.
Pekny, M., Eliasson, C., Siushansian, R., Ding, M., Dixon, S.J., Pekna, M., Wilson, J.X., Hamberger, A., 1999. The impact of genetic removal of GFAP and/or vimentin on glutamine levels and transport of glucose and ascorbate in astrocytes. Neurochem. Res. 24, 1357–1362.

Pekny, M., Nilsson, M., 2005. Astrocyte activation and reactive gliosis. Glia 50, 427–434.
Ren, C., Li, N., Wang, B., Yang, Y., Gao, J., Li, S., Ding, Y., Jin, K., Ji, X., 2015. Limb ischemic perconditioning attenuates blood-brain barrier disruption by inhibiting activity of MMP-9 and occludin degradation after focal cerebral ischemia. Aging Dis. 6, 406.
Sandoval, K.E., Witt, K.A., 2008. Blood-brain barrier tight junction permeability and ischemic stroke. Neurobiol. Dis. 32, 200–219.
Schiff, L., Hadker, N., Weiser, S., Rausch, C., 2012. A literature review of the feasibility of glial fibrillary acidic protein as a biomarker for stroke and traumatic brain injury. Mol. Diagn. Ther. 16, 79–92.
Shi, S., Qi, Z., Ma, Q., Pan, R., Timmins, G.S., Zhao, Y., Shi, W., Zhang, Y., Ji, X., Liu, K.J., 2017. Normobaric hyperoxia reduces blood occludin fragments in rats and patients with acute ischemic stroke. Stroke 48, 2848–2854.
Sofroniew, M.V., 2009. Molecular dissection of reactive astrogliosis and glial scar formation. Trends Neurosci. 32, 638–647.
Yang, G., Kitagawa, K., Matsushita, K., Mabuchi, T., Yagita, Y., Yanagihara, T., Matsumoto, M., 1997. C57BL/6 strain is most susceptible to cerebral ischemia following bilateral common carotid occlusion among seven mouse strains: selective neuronal death in the murine transient forebrain ischemia. Brain Res. 752, 209–218.
Yang, Y., Rosenberg, G.A., 2011. MMP-mediated disruption of claudin-5 in the blood–brain barrier of rat brain after cerebral ischemia. Claudins Methods Protoc. 333–345.
Yuan, S., Liu, K.J., Qi, Z., 2020. Occludin regulation of blood–brain barrier and potential therapeutic target in ischemic stroke. Brain Circ. 6, 152–162.
Yuan, Y., Zhang, Z., Wang, Z., Liu, J., 2019. MiRNA-27b regulates angiogenesis by targeting AMPK in mouse ischemic stroke model. Neuroscience 398, 12–22.